Size and Shape Dependent Catalytic Activity of Metal Nanoparticles as Co-catalyst for Metal – TiO_2 Photocatalysis

A

Thesis Submitted

in partial fulfillment of the requirements for the

Degree of

Master of Science in chemistry

Submitted by:

Ritu Bala

Reg. no.(300802016)

Under the Supervision of:

Dr. Bonamali Pal

Assistant Professor

School of Chemistry & Biochemistry

Thapar University

Patiala 147004

July 2010

Acknowledgement

I take this opportunity to pay my heartiest thanks to my guide Dr. Bonamali Pal for his guidance and support in doing my project work. He encourages and motivates me to learn more about the subject. I am grateful to Prof. Susheel Mittal for approving me for this project. I thank to Ms. Rupinder Makkar for her guidance. I thank to Mr. Rabindra Kumar Patel for his guidance and cool behavior. I thank to all the Research Scholars for their guidance and support to me. I also thank the laboratory staff for their timely help. I thank to all other faculty members and my friends for their help and motivation.

Date: 15/7/2010
Place: Thapar University,
Patiala

Ritu Bala
Ritu Bala

Candidate's Declaration

I hereby declare that the work being presented in the dissertation entitled **"Size and Shape Dependent Catalytic Activity of Metal Nanoparticles as Co-catalyst for Metal – TiO_2 Photocatalysis"** in partial fulfillment of the requirements for the award of the degree of Masters in Chemistry, School of Chemistry and Biochemistry (SCBC), Thapar University, Patiala, is my own work during the period of Jan to July 2010 under the supervision of Dr. Bonamali Pal. I have not submitted the matter embodied in this dissertation for the award of any other degree.

Patiala

Date: 15/7/2010

Ritu Bala

RITU BALA

This is to certify that the above statement made by the candidate is correct and true to the best of our knowledge

Dr. Bonamali Pal

Project Supervisor,

Assistant Professor (SCBC),

Thapar University

Sushil Mittal 15/7/10

Dr. Susheel Mittal

Head, (SCBC)

Thapar University

Certificate

This is to certify that the project entitled **"Size and Shape Dependent Catalytic Activity of Metal Nanoparticles as Co-catalyst for Metal–TiO_2 Photocatalysis"** being submitted by Ms Ritu Bala in partial fulfillment of the requirement for the award of degree of Master of Science in the School of Chemistry and Biochemistry, Thapar University, Patiala, is a bonifide work carried out under the supervision of Dr. Bonamali Pal and that no part of this project has been submitted for the award of any other degree by me.

Dr. Bonamali Pal,

Assistant Professor,

Thapar University

Head, 15/7/10

(Dr. Susheel Mittal)

School of Chemistry and Biochemistry,

Thapar University

Dean, Academic Affairs,

(Dr. R.K. Sharma)

Thapar University

4

LIST OF CONTENTS

1. INTRODUCTION

The synthesis of different shape and size of metal nanoparticles[1] and their optoelectronic properties becomes an active area of research. Coinage metal nanoparticles (NP's.) are the building blocks for the nanostructured materials. A particle whose size falls in the range of 1-100 nm is called a nanoparticle. Nanoparticles are of great scientific interest as they are effectively a bridge between bulk materials and atomic or molecular structures. Metal nanoparticles have a considerably higher percentage of atoms on their surface compared to bulk, which can make them more reactive. Particles in this dimension differ in many aspects compared to their bulk. Thus, the properties changes, as their size[2] approaches the nanoscale and as the percentage of atoms at the surface of a material becomes significant. For bulk materials, having size larger than one micrometer, the percentage of atoms at the surface is insignificant in relation to the number of atoms in the bulk of the material.

Gold in its bulk state is one of the most stable noble metals among group 8 elements which are resistant to oxidation. Because of its inertness, Au was formerly considered as an ineffective catalyst. But Haruta et al[3] have shown exceptionally high CO oxidation activity on supported nano Au catalysts even at sub-ambient temperatures (200 K). Nanosize particles of coinage metals are found to exhibit enhanced optical and catalytic activity. There are two major phenomena that are responsible for these differences: (i) High surface-to-volume ratio (ii) Quantum size[4] effect i.e. when the particle size decreases below the Bohr radius of the material used, the electron becomes more confined in the particle. This increases the band gap energy and the valence band and conduction bands break into quantized energy levels.

Brus Equation[5] showing the quantum confinement energy of the first excited electronic state:

$$E = E_g^{bulk} + \frac{h^2}{8r^2}\left[\frac{1}{m_0 m_e} + \frac{1}{m_0 m_h}\right] - \frac{1.8e^2}{4\pi€€_0 r}$$

From this equation, it is quite clear that if the particle radius is small, then the energy of the particle is very large. Here, E is the absorption onset inferred from UV spectra; E_g^{bulk} is the bulk band gap; h is Planck's constant; r is the particle radius; m_e and m_h are the effective mass of electrons and holes respectively ; m_0 and e are the mass and charge of a free electron, respectively; € is the relative permittivity and $€_0$ is the permittivity of free space.

Surface Plasmon band is the characteristic feature of the metal nanoparticles. SP band arises because of the interaction of the light radiation with the free electrons present in the conduction band. When the wavelength of light is much larger than the nanoparticle size, it can set up resonance condition. Light in resonance with the surface Plasmon oscillation causes the free electron in the metal to oscillate and give rise to SP band. The oscillation frequency is usually in the visible region for gold, silver and copper giving rise to the strong surface Plasmon resonance absorption. For example, SP band of gold nanoparticles appear at 520 nm, for silver nanoparticles appear at 420 nm and copper nanoparticles at 570 nm. These are the fundamental absorption bands of the metal nanoparticles. The frequency of the SP resonance depends on no. of factors such as particle size, shape and the nature of the surrounding medium. If the size of the metal nanoparticles increases, the SP band shifted towards right i.e. red shift[5] takes place. For nanorods[6,7], the SP resonance splits into two bands: parallel (longitudinal) and perpendicular (transverse) to the axis of the nanorods. Change in the absorbance or wavelength gives a measure of the particle size, shape, and interparticle properties. Polar solvent addition to metal nanoparticles shifts the band towards higher wavelength because of the dipole-dipole interaction.

All the metal nanoparticles do not show SP band. Many metals such as, Pt, Rh, Pb, In, Hg, Cd and Sn etc. the surface plasmon frequency lies in the UV part of the spectrum and these nanoparticles do not display strong color effects. Such metal nanoparticles get readily oxidized. So, surface plasmon study of such metal nanoparticles is quite difficult. But the coinage metals such as Au, Ag and Cu are exceptional. The preliminary characterization of such nanoparticles is through SP band. These metals are noble and form air stable colloids except the case of Cu nanoparticles[8]. These metals have d-electrons and because of these d-electrons, d-d band transition occurs and the plasmon frequency is pushed into the visible part of the spectrum. So, the surface plasmon studies are most commonly carried out with Au, Ag and Cu[9-12] There are a number of applications of metal nanoparticles are known till date[1-2,13] Metal nanoparticles show their application in thermal catalysis, biosensor, electronic devices, separation technology, and as a biocatalyst[14] in many medicines to cure diseases and photocatalysis.[15-20]

Photocatalysis is one of the most important applications of coinage metal nanoparticles. Photocatalysis is the acceleration of a photoreaction in the presence of a catalyst or a change in the rate of chemical reactions or their generation under the action of light in the presence of

substances called photocatalysts that absorb light quanta and are involved in the chemical transformations of the reaction participants. Semiconductor -metal composites shows a very interesting property in the field of photocatalysis. The metal in contact with the semiconductor greatly enhances the overall photocatalytic efficiency. Photoexcited semiconductor nanoparticles undergo charge equilibration when they are in contact with metal nanoparticles. Metal ion doped semiconductor composites exhibit shift in the Fermi level to more negative potentials. The shift in the Fermi level[16] depends upon the size of the metal nanoparticle.

1.1 MECHANISM OF PHOTOCATALYSIS

The basic principles of heterogeneous photocatalysis can be summarized shortly as follows. A semiconductor (SC) is characterized by an electronic band structure (Fig-1) in which the lowest occupied energy band, called valence band (VB), and the highest empty band, called conduction band (CB), are separated by a bandgap[4,21], i.e. a region of forbidden energies in a perfect crystal. When a photon of energy higher or equal to the band gap energy is absorbed by a semiconductor particle, an electron from the VB is promoted to the CB with simultaneous generation of a hole (h^+) in the VB. The e^- of CB and the h^+ of VB can recombine on the surface or in the bulk of the particle in a few nanoseconds or can be trapped in surface states where they can react with donor (D) or acceptor (A) species adsorbed or close to the surface of the particle. Thereby, subsequent anodic and cathodic redox reactions can be initiated. The photogenerated h^+ is strongly oxidizing and can oxidize all the organic chemicals to CO_2 and H_2O etc. The energy level at the bottom of the CB is actually the reduction potential of photoelectrons and the energy level at the top of the VB determines the oxidizing ability of holes, each value reflecting the ability of the system to promote reductions and oxidations.

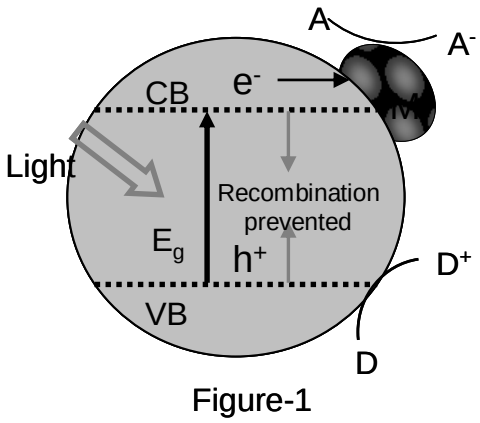

Figure-1

Principle of Photocatalysis

The flatband potential, $V_{fb,}$ locates the energy of both charge carriers at the SC–electrolyte interface, and depends on the nature of the material and the system equilibria. From a thermodynamic point of view, adsorbed couples can be reduced photocatalytically by CB electrons if they have redox potentials more positive than the V_{fb} of the CB, and can be oxidized by VB holes if they have redox potentials more negative than the V_{fb} of the VB. The efficiency of a photocatalyst depends on the competition of different interface transfer processes involving electrons and holes and their deactivation by recombination[22].

1.2 How metal Co-catalysts help in improving the Photocatalytic activity of semiconductors

The common methods for facilitating electron transfer from conduction band electrons to solution species has been through the use of metal island co-catalysts deposited onto the photocatalysts surface. These metal islands mediate multielectron redox processes with solution phase redox carriers, and enhancements of both anodic and cathodic redox processes have been observed at illuminated semiconductor electrodes that have metal island deposits. Small metal islands of Ag, Au, and Cu can be deposited onto the TiO_2 surface photo-chemically. Metal-semiconductor nanocomposite which results in the drastic increase in the activity of semiconductor by equilibrating the Fermi energy levels of both identities resulting in the easy transference of electrons from CB of semiconductor to metal[23].

Deposition of metal on semiconductor enhances the efficiency of photocatalytic redox processes. Generally the coinage metal nanoparticles are used for this purpose. The size-dependent shift in the apparent Fermi level of the TiO_2- Au composite shows the ability of Au nanoparticles to influence the energetics by improving the photoinduced charge separation. Metal ion doped semiconductor composites exhibit shift in the Fermi level to more negative potentials. Such a shift in the Fermi level improves the energetics of the composite system and enhances the efficiency of interfacial charge-transfer process.

With the reduction in the size of metal particles that are attached to TiO_2 (scheme below), Fermi level shifts more towards the negative direction i.e. towards the conduction band which further helps in easy transfer of electrons from semiconductor to metals and improve the photoinduced redox reactions. As the deposited (onto TiO_2) metal particles size gradually

decreases, the photocatalytic enhancement of TiO_2 also highly increases. Also the shape of the metal co-catalysts particles used for the metal-TiO_2 junction, may changes the photoinduced charge transfer processes and thereby it is expected to alter the photocatalytic activity of TiO_2.

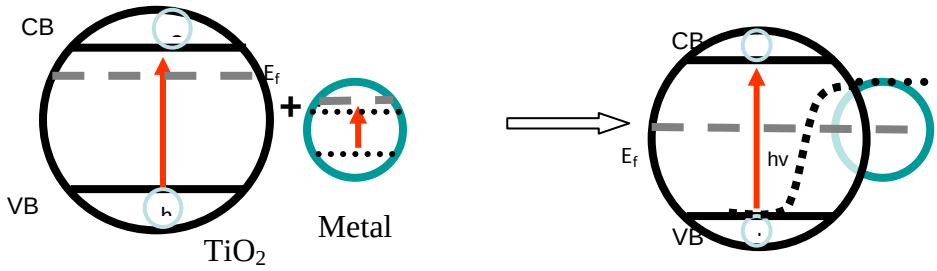

Fig. 2 Fermi level Equilibrium between TiO_2-Metal (Au, Ag & Cu)

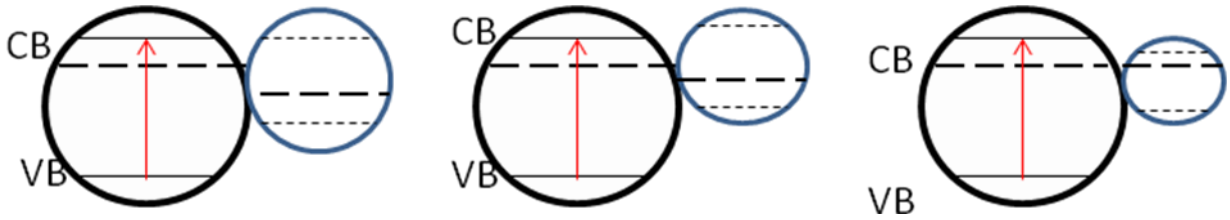

Fig. 3 Fermi level shifts towards more negative potential with the decrease in size of metal co-catalysts nanoparticles.

1.3 Synthesis and Applications of coinage metal nanoparticles

Coinage metal nanoparticles were synthesized by the seed-mediated growth method. In this method, the size of nanoparticles can be controlled by varying amount of reducing agent and surfactant. Nanosize particles of coinage metals are found to exhibit enhanced optical and catalytic activity due to their small size and high surface-to-volume ratio. So, the nanoparticles of coinage metals show interesting applications in the field of photocatalysis[24-26]. Metal nanoparticles such as gold and silver shows catalytic activity in many chemical reactions. Although gold[27] is inert of all metallic elements yet it has interesting applications as a co-catalyst[28].

2.OBJECTIVE

1. Synthesis of coinage metal (Au, Ag and Cu) nanoparticles and their characterization using spectroscopic techniques and TEM size analysis
2. Effect of different solvents on the aggregation on Au nanoparticles.
3. To study the size & shape dependent catalytic activity of these prepared co-catalyst for the metal-TiO_2 photocatalytic degradation of organic compounds, e.g., Salicylic acid, Benzoic acid.
4. Comparative study of photocatalytic activity of TiO_2 by adding different size and shape of various coinage metal nanoparticles.

3. EXPERIMENTAL WORK

3.1 Synthesis of different shapes and sizes of metal nanoparticles

Synthesis of Gold Nanoparticles:

Materials used: $HAuCl_4.3H_2O$ (Aldrich), Ascorbic acid (Aldrich), $NaBH_4$ (RANKEM), Silver nitrate, cetyltrimethylamoniumbromide (CTAB) (Aldrich) was used as received. Deionized water was used for all solution preparations. Gold nanoparticles were prepared in aqueous solution by seed mediated method. This method comprises of two steps:

(i) Preparation of seed solution: It contains $HAuCl_4$ (0.01M) (250µl), $NaBH_4$ (0.01M) (600 µl) and cetyltrimethylamoniumbromide (CTAB) (0.1M) (9.5 ml) under 0˚C conditions. Stirred this mixture solution for two minutes.

(ii) Preparation of Growth Solution: It contains $HAuCl_4$ (0.01M) (500µl), $AgNO_3$ (75µl) Ascorbic acid (0.1M) (55µl) and cetyltrimethylamoniumbromide (CTAB) (0.1M) (9.5 ml) and 12 µl of seed solution was added into the growth solution. The resulting colloidal solution appears to be purple in color and studied their optical properties by UV spectrophotometer and TEM size analysis.

Formation of gold nanorods: Gold nanorods were prepared by the same method as for the gold nanoparticles. The only difference is that the seed solution and the growth solution are kept at 40 ^oC. At higher temperature the gold nanoparticles were transformed into gold nanorods.

Synthesis of Silver Nanoparticles: This method involves the addition of mixture solution of cetyltrimethylamoniumbromide (CTAB) (0.1M) (9.5ml) and $NaBH_4$ (0.01M) (1ml) to the mixture solution of cetyltrimethylamoniumbromide (CTAB) (0.1M) (9.5ml) and $AgNO_3$ (0.01M) (1ml). This resulting solution appeared yellowish in color and characterized by UV spectroscopy.

Synthesis of Copper Nanoparticles: This method involves the addition of mixture solution of cetyltrimethylamoniumbromide (CTAB) (0.1M) (9.5ml) and $NaBH_4$ (0.01M) (1ml) to the mixture solution of cetyltrimethylamoniumbromide (CTAB) (0.1M) (9.5ml) and $Cu(NO_3)_2$ (0.01M) (1ml). The pH of the latter solution was maintained highly basic by adding NH_3 solution to it. This resulting solution appeared dark brown in color and characterized by UV spectroscopy.

3.2 Photocatalytic Reactions

Photocatalytic efficiency was investigated by photocatalytic degradation of Salicylic acid and Benzoic acid by addition of these as-prepared metal nanoparticles to TiO_2 suspension under light irradiation from UV light (10.4 mW). Typically, 5 ml aqueous suspension of organic compounds and 50 mg TiO_2 (Degussa, P25) was taken in a test tube and required amount of coinage metal nanoparticles solution was added to it for making M-TiO_2 composite and irradiated under magnetic stirring for various time periods and the concentration of the degraded salicylic acid and benzoic acid were analyzed by the measurement of absorbance spectra at 298 nm and 273 nm (wavelength of maximum absorption), respectively. Photocatalytic efficiency of metal Co-catalysts was verified by the following experimental procedure.

(a) Effect of TiO_2 concentration on metal Co-catalysts addition

In this method we have taken the different amounts of TiO_2 (from 10 mg to 300 mg) by keeping the amount of Au/Ag nanoparticles constant. To check the photocatalytic degradation of salicylic acid and benzoic acid, we have taken 5 ml. of aqueous solution of the organic compound, different amounts of TiO_2 and a constant amount of Au and Ag nanoparticles. This mixture was light irradiated under magnetic stirring for different time periods. The reaction product was analysed by UV spectrophotometer.

(b) Effects of the amount of Au/Ag nanoparticles loading to TiO_2

In this method we have varied the amounts of Ag/Au NPs (from 10 µl to 300 µl) by keeping the amount of TiO_2 constant. To check the photocatalytic degradation of salicylic acid and benzoic acid, we have taken 5 ml. of aqueous solution of the organic compound, different amounts of TiO_2 and a constant amount of Au and Ag nanoparticles. This mixture was light irradiated under magnetic stirring for different time periods. The reaction product was analysed by UV spectrophotometer.

3.3 Characterization of Coinage Metal Nanoparticles

Surface Plasmon band (SP) is the preliminary characterization of metal nanoparticles. We can estimate the size of metal NP's from the position of SP band. If SP band of gold nanoparticles appear at 520 nm, the size range of the NP's is about 2-3 nm, as reported. As the size[29] of the metal nanoparticles increases, the SP band shifts towards the higher wavelength i.e. red shift took place. For silver nanoparticles SP band appear at 420 nm and copper nanoparticles at 570 nm. These are the fundamental absorption bands of the metal nanoparticles. After the addition of polar solvent to Au NP's, aggregation of the nanoparticles takes place and results in the formation of a new band at 970-980 nm where as non polar solvent addition (CCl_4) does not aggregate the Au NPs.

For measurement of Au nanoaprticles size, Transmission electron microscope (TEM) images were taken using a Hitachi 7500 transmission electron microscope having power 120 KV. The following TEM images confirms the formation of spherical Au NP's (size 3 nm) in Fig. 4(a), Au nanorods (20 nm) in (b) & (c) , Aggregated Au NP's (15 nm) which show chain like formation in Fig. 4(d) (e) & (f) after the addition of methanol.

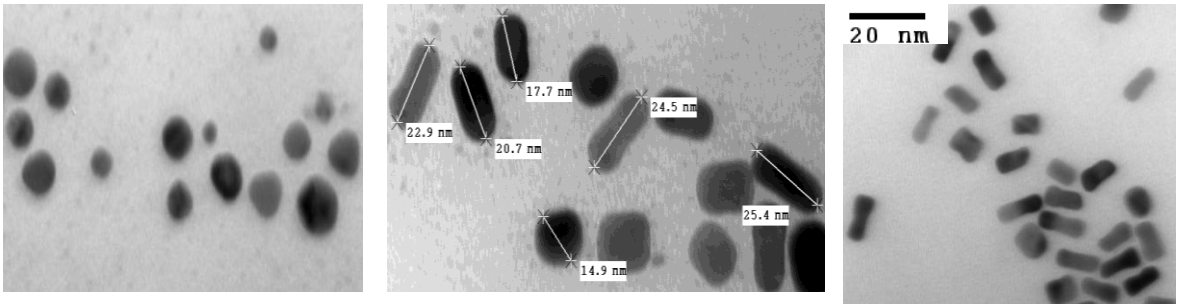

(a) **(b)** **(c)**

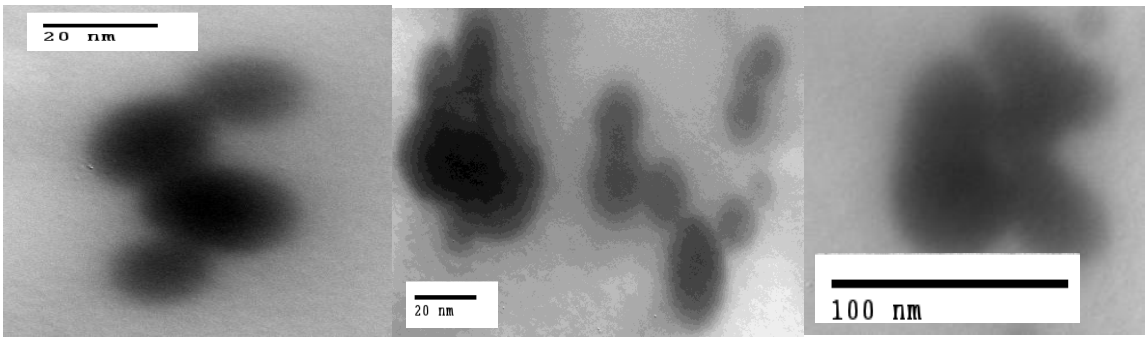

(d) **(e)** **(f)**

TEM images of various Au nanoaprticles of different shape and size

4. RESULTS AND DISCUSSION

(i) Optical properties of Coinage Metal Nanoparticles of different Shape and Sizes

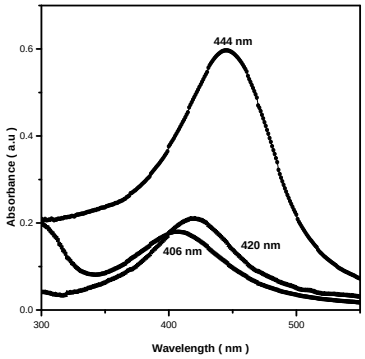

Fig.4 SP bands Vs sizes of Silver NP's

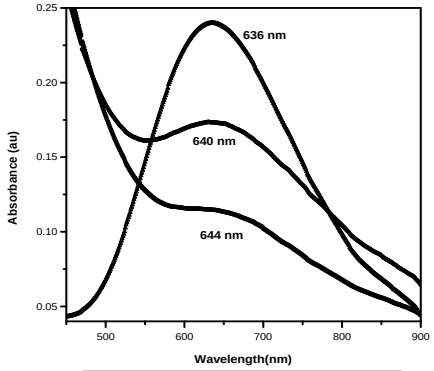

Fig.5 SP bands Vs sizes of Copper NP's

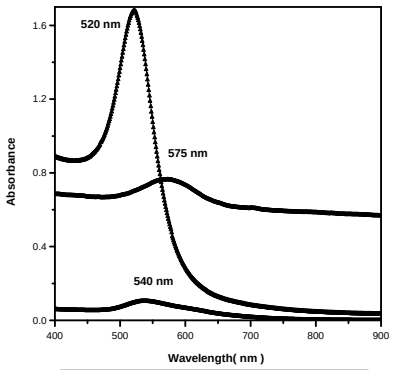

Fig.6 SP bands Vs sizes of Au NP's

Fig.4-6 showed the surface Plasmon absorption band of Cu (λ_{max}: ~ 630-650 nm, size range: ~ > 10 - 20 nm), Ag (λ_{max} : 421 nm, size : < 10 nm) and Au (λ_{max}: ~ 521, 540 & 573 nm, size range: ~ 10 - 20 nm) nanoparticles which is red shifted due to increasing size of nanoparticles. In Fig.7, Au nanorods show two surface plasmon bands, one around λ_{max}: 540 nm and the other at around λ_{max}: 800nm compared to one SP band (540 nm) of spherical Au NPs.

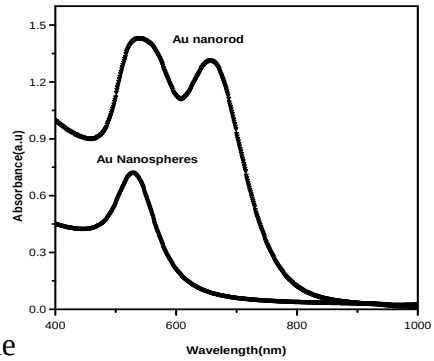

Fig.7 SP bands Vs shapes of Au NP's

(ii)Effect of different Solvents on the Au NP's.

The Fig. 8 shows the effect of various solvents addition to the aqueous solution of Au nanoparticles. It was found that on the addition of polar solvents [Fig. 8(a)], a new characteristic SP band which appeared at 970-980 nm along with the existing conventional band at 540 nm. This aggregation is due to dipole-dipole interaction between the polar solvents and Au NP's. The results further confirmed by the addition of non-polar solvent (CCl_4) that do not show any new peak at 970 nm as shown in Fig. 8(b), indicating that aggregation of Au NPs is not occurring in this solvent due to absence of charge dipole.

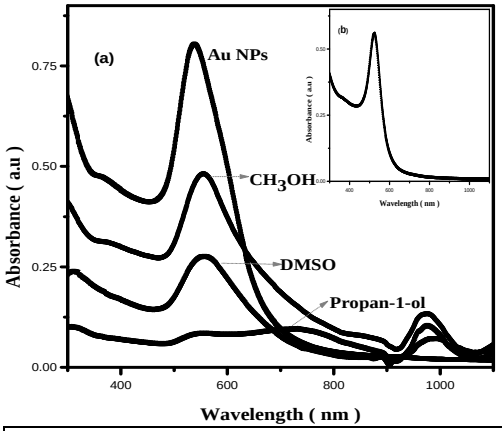

Fig. 8 (a) Addition of polar solvents to Au NP's
(b) Addition of non-polar (CCl_4) solvent

(iii) Measurement of catalytic activity of different shapes and sizes of Au NP's through photoactivity of metal-TiO_2 junction formation.

Different shape and sizes of Au nanoparticles showed different catalytic activity. It was verified from Fig.9 which showed the time course of salicylic acid degradation by adding different shape and sizes of metal co-catalysts. The photocatalytic activity was highly enhanced by addition of Au nanoparticles to TiO_2 as compared to bare TiO_2. It is seen that Au non-aggregated NP's (size 3 nm) addition to TiO_2 exhibits highest activity than aggregated NP's (size 15 nm) addition. Similarly, Au photodeposited TiO_2 showed lower activity compared to nanoparticle addition because of large aggregation of Au particles deposits/islands on TiO_2 surface during photodeposition. Also, Au nanorods addition to TiO_2 photocatalysis decreases the photoactivity as compared to spherical Au nanoparticles addition. It is proved that photocatalytic activity gets

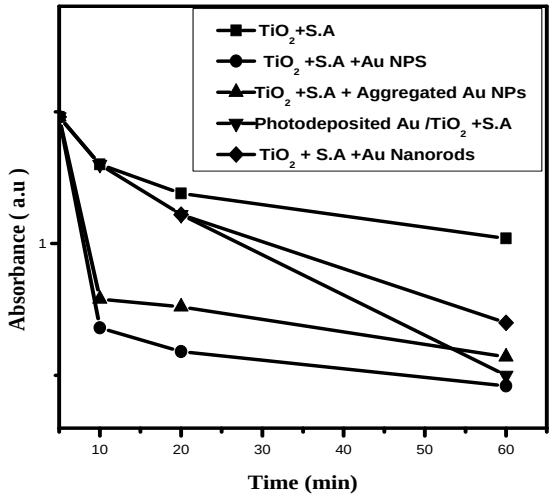

Fig. 9 Photocatalytic activity of different shapes and sizes of Au NP's

enhanced by adding calculated amount of separately synthesized non-aggregated spherical nanoparticles to TiO_2 photocatalyst compared with Au photodeposition onto TiO_2 and Au nanorods–TiO_2 junction which probably due to different rate of photoinduced charge transfer processes and Fermi energy level equilibrium as a function of various size and shape of Au particles.

(iv) Photodegradation of Benzoic acid by varying the amount of Au NPs

It was observed that by addition of Au metal co-catalyst to TiO_2 photocatalyst, rate of photodegradation is increased, but this increase is only up to a certain extent of Au NPs concentrations. By varying the amount of Au NPs (10 µl - 200 µl) and taking the TiO_2 (10 mg) constant, we concluded that on the addition of 10-50 µl Au NPs, the rate of photocatalytic activity was maximum. As seen from the graph that further addition of Au NP's ca. 100- 200 µl, the rate of photodegradation of Benzoic acid is decreased due to higher surface coverage of Au NP's on the TiO_2 surface which prevents the penetration of proper amount of light for the photoexcitation of TiO_2, resulting in the decrease rate of electron-hole pair generation retarding the photooxidation activity.

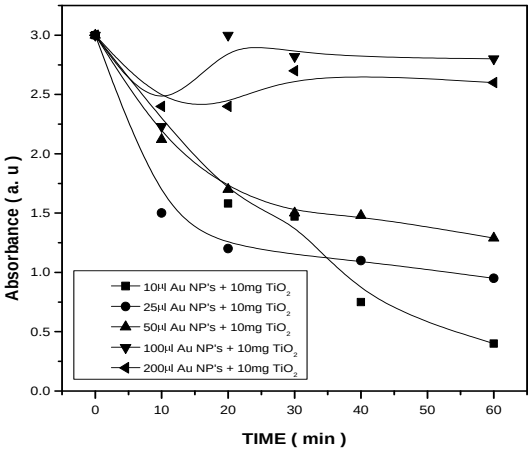

Fig. 10 Photodegradation of benzoic acid by varying amounts of Au NP's.

(v) Photodegradation of Salicylic acid by varying the amount of Au NP's

The above result was further confirmed by taking Salicylic acid instead of Benzoic acid. In this graph, it was observed that addition of Au metal co-catalyst to TiO_2 photocatalyst, rate of photodegradation was increased, but this increase is

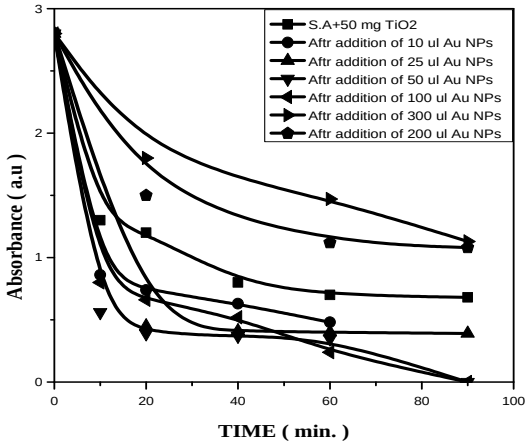

Fig. 11 Photodegradation of salicylic acid by varying amounts of Au NP's.

only up to a certain extent up to 100 µl Au NPs addition. By varying the amount of Au NP's and taking the TiO_2 (50 mg) constant, it was concluded on the addition of 100 µl Au NP's, the rate of photocatalytic activity is the maximum. Furthermore addition of Au NP's (200-300 µl) to TiO_2, the rate of photodegradation of salicylic acid is further decreased.

(vi) Photodegradation of Salicylic Acid by varying amount of TiO_2

The photodegradation of salicylic acid was observed by varying the amount of TiO_2 (10 mg to 100 mg) and keeping the Au NP's constant (100 µl). It was revealed from the Fig. 12 that on increasing the amount of TiO_2 photocatalyst, the rate of photodegradation of salicylic acid is gradually increased because higher amount of salicylic acid gets adsorbed on the surface of large number of TiO_2 particles which forms a chelating complexes and instantly degraded by the photogenerated holes on light irradiation.

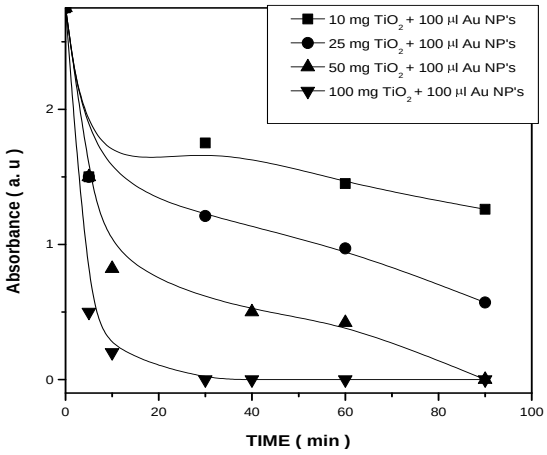

Fig. 12 Photodegradation of salicylic acid by varying the amounts of Au NPs

(vii) Photodegradation of Benzoic Acid by Ag NP's addition to TiO_2

As discussed above, on increasing the amount of TiO_2 photocatalyst and keeping the amount of Ag metal co-catalyst constant, the rate of photodegradation is enhanced. It was observed from Fig. 13, by increasing the amount of TiO_2 and keeping the amount of Ag NP's constant, the rate of photocatalytic degradation of benzoic acid is increased.

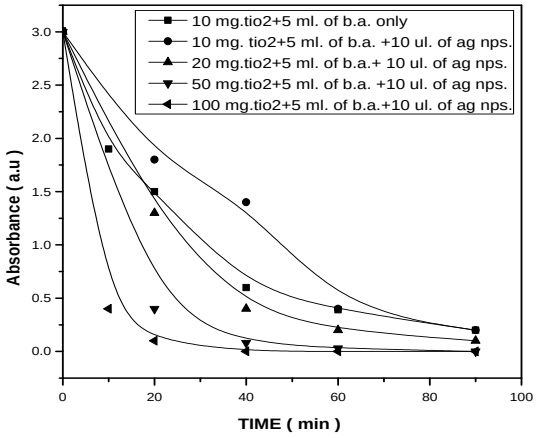

Fig. 13 Photodegradation of benzoic acid by varying the amounts of TiO_2

5. CONCLUSION

It is concluded that by adding different shape and sizes of metal co-catalysts to TiO_2 photocatalyst, there is always enhancement in the rate of photocatalytic activity. The photocatalytic activity was maximized by addition of Au nanoparticles of different morphology and nature as compared to bare TiO_2. It can also be seen that Au non-aggregated NP's (size 3 nm) addition to TiO_2 exhibits highest activity than aggregated NP's (size 15 nm) addition. Similarly, Au photodeposited TiO_2 showed lower activity compared to nanoparticle addition because of large aggregation of Au particles formed on TiO_2 surface during photodeposition. Also, Au nanorods addition to TiO_2 photocatalysis decreases the photoactivity in degrading salicylic acid compared with Au nanoparticle addition. An appreciable difference in the photocatalytic activity was observed by the addition of different shapes of nanoparticles (spherical and rod shape).

A very interesting observation is the photocatalytic enhancement of rate of degradation of salicylic acid and benzoic acid by the addition of different shape and size of NP's only up to a certain extent. On exceeding a certain limit, the photocatalytic activity decreased and this decrease is due to the accumulation of Au NP's on the TiO_2 surface which prevents the penetration of adequate amount of light for the photoexcitation of electrons from the conduction band and retards the generation of holes in valence band of TiO_2 and thereby decreasing the oxidation pathways. On increasing the amount of TiO_2 photocatalyst, the rate of photodegradation of salicylic acid and benzoic acid is increased because of higher adsorption of salicylic acid and benzoic acid occurs on the surface of large number of TiO_2 particles.

6. REFERENCES

1. S. Eustis, M. A. El-Sayed, *Chem. Soc. Rev.*, **2006**, 35, 209-217.
2. M. C. Daniel, D. Astruc, *Chem. Rev.*, **2004**, 104, 293-346.
3. A. L. Linsebigler, G. Lu, J. T. Yates, *Chem. Rev.*, **1995,** *95*, **735-758.**
4. M. I. litter, *Appl. Catalysis. B, Environ.,* **1999**, 23, 89-114.
5. R. Lv, C. Cao, Y. Guo, H. Zhu, *J. Mater. Sci*., **2009**, 39, 1575-1578.
6. I. Lisiecki, *J. Phys. Chem. B.*, **2005**, 109, 12231-12244.
7. I. D. Dragieva, Z. B. Stoynov, K. J. Klabunde, *Scripta Mater.*, **2001**, 44, 2187-2191.
8. M. Samin, N. K. Kaushik, A. Maitra, *Bull. Mater. Sci*., **2007**, 30, 535-540.
9. L. L. Zhao, K. L. Kelly, G. C. Schat, *J. Phys. Chem. B.*, **2003**, 107, 7343-7350.
10. S. D. Solomon, M. Bahadory, A. V. Jeyarajasingam, S. A. Rutkowsy, C. Boritz, *J. Chem. Edu.*, **2007**, 84, 322-325.
11. T. Nagareda, S. Hayashi, K. Yamamoto, *Phys .Rev. B.*, **1991**, 44, 3125-3129.
12. P. Christopher, S. Linic, *J. Am. Chem. Soc.*, **2008,** 130, 1676-1680.
13. D. Syroka, V. Kasicka, I. Miksik, P. Rezanka, K. Zaruba, P. Matejka, V. Kral, *J. Sep. Sci.*, **2010**, 33, 372-387.
14. C. W. Corti, R. J. Holliday, D. T. Thompson, *Appl. Catalysis. A*: *Gen.*, **2006,** 38, 231-240.
15. D. Buso, J. Pacifico, A. Marucci, P. Mulvany, *Adv. Func. Mater.*, **2007**, 17, 347-354.
16. V. Subramanian, E. E. Wolf, P. V. Kamat, *J. Phys. Chem. B*, **2007**, 105, 4943-4950.
17. H. Li, Z. Bian, J. Zhu, Y. Huo, H. Li, Y. Lu , *J. Am. Chem. Soc.*, **2007**, 129, 4538-4539.
18. J. A. Rodriguez, G. Liu, T. Jirsak, J. Hrbek, Z. Chang, J. Dvorak, A. Maiti, *J. Am. Chem. Soc.*, **2002**, 124, 5242-5250.
19. G. R. Bamwenda, S. Tsubota, T. Nakamura, M. Haruta, *Catal. lett.*, **1997**, 44, 83-87.

20. A. Dawson, P. V. Kamat, *J. Phys. Chem. B.*, **2001**, 105, 960-966.

21. P. V. Kamat , *J. Phys. Chem. B*, **2002**, 106, 7729-7744.

22. A. Dawson, P. V. Kamat, *J. Phys. Chem. B.*, **2001**, 105, 960-966.

23. A. Wood, M. Giersig, P. Mulvaney, *J. Phys. Chem. B.*, **2001**, 105, 8810.

24. K. Hashimato, H.Irie, A. Fujishima, *J. Appl. Phys.*, **2005,** 44, 8269–8285.

25. P. Dube, F. D. Toste, *J. Am. Chem. Soc.,* **2006**, 128, 12062-12063.

26. S. Link, C. Burda, B. Nikoobakht, M. A. El-Sayed, *J. Phys. Chem. B.*, **2000**, 104, 6152-6163.

27. M. B. Cortie1 and E. V. Lingen, *Mater. Forum.*, **2002,** 26, 1-14.

28. C. W. Corti, R. J. Holliday, D. T. Thompson, *Appl. Catal. A: Gen.*, **2005**, 44, 331-343.

29. L. M. L. Marzan, *Langmuir.,* **2006,** *22,* 32-41.